IX CONGRESSO BRASILEIRO DE ENGENHARIA E CIÊNCIAS TÉRMICAS
9th BRAZILIAN CONGRESS OF THERMAL ENGINEERING AND SCIENCES

Paper CIT02-0759

NACELLE DESIGN FOR AERONAUTICAL ENGINES

Cláudio Sade Brodt
EMBRAER – Empresa Brasileira de Aeronáutica
Av. Brigadeiro Faria Lima, 2170, PC 191, 12227-901 - São José dos Campos - SP, Brazil
claudio.brodt@embraer.com.br

Guilherme Lara Oliveira
EMBRAER – Empresa Brasileira de Aeronáutica
Av. Brigadeiro Faria Lima, 2170, PC 191, 12227-901 - São José dos Campos - SP, Brazil
guilherme.oliveira@embraer.com.br

João Roberto Barbosa
Instituto Tecnológico de Aeronáutica
CTA/ITA/IEM/IEME - 12228-900 - São José dos Campos - SP, Brazil
barbosa@mec.ita.br

Abstract. *The nacelle design and integration with the aircraft is a key point in the overall aircraft design. The nacelle inlet must deliver the mass flow required by the engine to develop the necessary thrust at all flight envelope. Minimum variations in the inlet capture area, the inlet profile and the nozzles exit areas may have a great influence in the flow properties, compromising the engine performance. Although some theoretical and empirical methods are used nowadays to design nacelles with reasonable performance, they are not usually available in the open literature, due to its technological importance in the aerospace industry. So, the main motivation of this paper is to evaluate the proposed methodology for subsonic nacelles design and check the basic performance for specific engines. The method is divided in three steps: the hardpoints estimation, which satisfy the specific conditions required by the engine, the aerodynamic profile design, which must be smooth and suitable, and the CFD analysis to check and improve.*

Key Words: *Aircraft, Nacelle, Design, CFD.*

1. Introduction

The engine is responsible for delivering the necessary thrust to the airplane at all operational conditions. To achieve this, it requires different amounts of air mass flow at each flight condition, which is delivered by a suitable nacelle. It must also yield enough room for all engines build up unit (EBU) and protect the turbomachinery from foreign objects ingestion (FOI) and impact. An appropriate method to nacelle design is very important in order to assure engine requirements and so overall aircraft performance.

The nacelle design may be divided into four main steps: the inlet capture-area estimation, the inlet profile definition, the exit areas determination and the exhaust profile lofting definition. Minimum variations in any of these parts may have a great influence in the flow properties, compromising the engine performance.

Despite its technological importance for the aerospace industry, the open literature lacks a clear, complete and detailed nacelle design method. Some empirical and statistical formulae are known but their generality are not suitable for specific design applications, limiting their application to check analysis.

This paper summarizes the work done by Brodt, 2001, whose main motivation was to develop a new design methodology for subsonic civil nacelles equipped with specific engines to assure the design aircraft performance at all flight conditions. The EMBRAER new regional jet ERJ-170 was chosen as a case study to evaluate the methodology. The results were compared to existing nacelle and with others obtained from statistical approaches.

The purposed method is divided basically into three steps. Firstly, to determine all nacelle geometry points, called hardpoints, to match engine requirements. Inlet and exit areas dimensions are determined from momentum conservation theorem and continuity. Engine dimensions and further assumptions will give the intermediate points. Then, a smooth and convenient aerodynamic profile will be fitted to those points using CAD tools. Finally, a CFD analysis will be iteratively carried out in order to improve the nacelle performance.

2. Theoretical Approach

Typically, the propulsion system is divided into three main parts, the engine, the nacelle inlet system and the nacelle exhaust system, which will be analyzed separately in this section, details of which may be seen in Mattingly, 1987. The nacelle is considered as isolated and the flow axis-symmetric.

2.1 Engine

The EMBRAER ERJ-170 is equipped with two underwing GE short duct high bypass turbofan engines, CF34-8 model (3.25m length, 1.17m fan diameter, bypass ratio 5, 63165N maximum thrust). Sometimes, it is possible that the engine main characteristics are not known at the beginning of the nacelle design. Engine design information such as types, positioning and dimensioning may be found, for instance, in Oates, 1989a, Oates, 1989b, Roskam, 1997 and Raymer, 1999.

2.2 Inlet System

The engine is surrounded by cowls, which protect its components and provide smooth surfaces for clean airflow, internally and externally. The inlet system is part of the nacelle.

Subsonic installations are easier to design because a simple fixed geometry is able to capture a wide range of flow. The inlet system most important parameter, the throat area, must satisfy the maximum engine flow requirement. It must be minimum to minimize drag, weight and cost and consistent with the specified internal performance (pressure recovery) and stability (pressure distortion). In practice, the free stream flow must be first slowed down by the inlet system to a speed of about Mach 0,4 to 0,7 to keep the compressor blades tip speed below sonic speed. Pressure loss and distortion of the air supplied to the engine affect the installed thrust and the fuel consumption. 1% reduction in the inlet pressure recovery, the ratio between engine and free stream total pressures, may reduce the thrust up to 1,3%.

The Pitot, or normal shock inlet (NSI), is suitable for high subsonic applications. The inlet radius for a given maximum operational Mach number is calculated from Eq. (1) and it can be compared to initial layout estimates from Fig. (1) (Raymer, 1999).

$$\frac{A_{throat}}{A_{engine}} = \frac{\left(\frac{A_{throat}}{A^*}\right)}{\left(\frac{A_{engine}}{A^*}\right)} = \frac{\frac{1}{M_{throat}}.\left[\frac{2}{\gamma+1}.\left(1+\frac{\gamma-1}{2}.M_{throat}^2\right)\right]^{\frac{(\gamma+1)}{2.(\gamma-1)}}}{\frac{1}{M_{engine}}.\left[\frac{2}{\gamma+1}.\left(1+\frac{\gamma-1}{2}.M_{engine}^2\right)\right]^{\frac{(\gamma+1)}{2.(\gamma-1)}}} = \frac{M_{engine}}{M_{throat}}.\left[.\frac{2+(\gamma-1).M_{throat}^2}{2+(\gamma-1).M_{engine}^2}\right]^{\frac{(\gamma+1)}{2.(\gamma-1)}} \quad (1)$$

where M is the aircraft flight envelope maximum operational Mach number at the indicated position, γ is the specific heats ratio, A^* is the throat area.

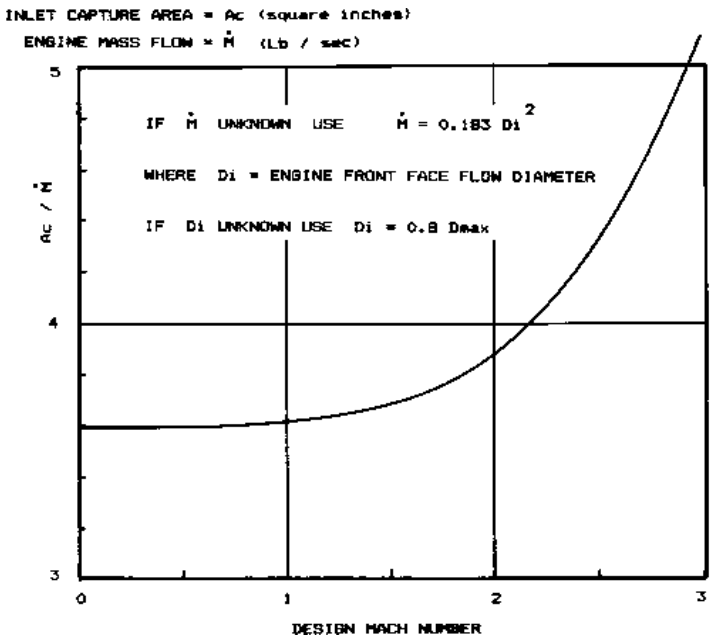

Figure 1. Capture area estimation

Another important parameter concerning inlet design is the length of the diffuser, which is the internal part of an inlet, where the free stream flow is slowed down to the speed required by the fan. For long diffusers, it is important to verify that the cross sectional area is smoothly increasing from the throat to the engine. For subsonic aircrafts, the diffuser should be as short as possible, without exceeding an internal angle of about 10^o, and this usually points out for a PITOT inlet with a length approximately equal to its front face diameter. In general, practice shows that the nacelle maximum diameter tends to be roughly 10% greater than the bare engine to accommodate many engine systems. The

inlet itself extends about 60% of the diameter in front of the fan face and the inlet area is about 70% of the maximum area, although depending on the engine type. Important parameters to check diffusers efficiency are the stagnation pressure ratio r_d and the isentropic or kinetic efficiency η_{kd}, shown in Eq. (2a, b) and described in details in Hill, 1970.

$$r_d = \left(\frac{P_{T,fan}}{P_{T,\infty}} \right) \text{ and } \eta_{kd} = \frac{r_d \cdot \left(1 + \frac{\gamma - 1}{2} . M^2 \right)^{\frac{\gamma - 1}{\gamma}} - 1}{\frac{\gamma - 1}{2} . M^2} \tag{2a, b}$$

where $P_{T,\infty}$ is the total pressure of the free stream flow.

The model proposed for the nacelle theoretical analysis is based on an aerodynamic duct in an air stream flow. The main stations of the flow are shown in Fig. (2): the first station, ∞, is at the undisturbed flow stream, station c is the duct entry, station f is the engine-face and station e is the duct exit. The internal cross-sectional area at station f, A_f, is known from the engine fan. Capture area A_c is determined first. It controls how much flow goes through the duct. Further details are found in Seddon, 1985.

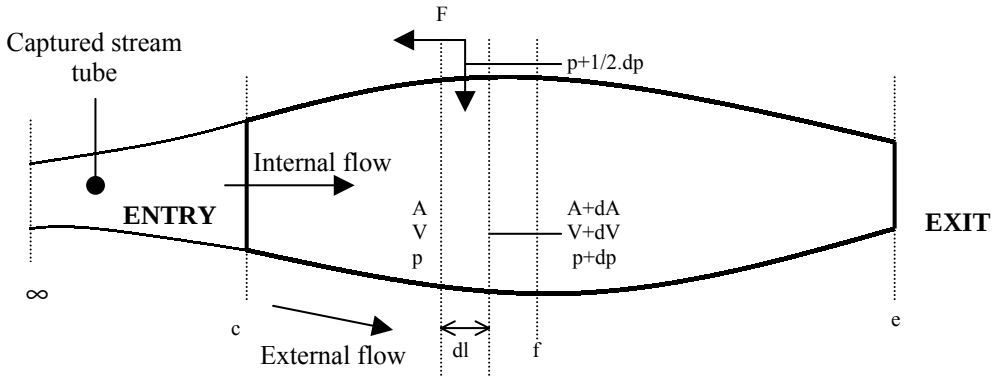

Figure 2. Aerodynamic duct in an air stream

Assuming uniform conditions of pressure and velocity at each station, a very small stream tube boundary inclination to its axis, total pressure loss caused essentially by friction on the walls of the duct and no compressibility effect in kinetic pressure on approach, the momentum conservation equation, Eq. (3), gives an approximate expression, Eq. (4), for the total pressure loss along the tube.

$$\rho . A V . (V + dV - V) = P_S . A + \left(P_S + \frac{1}{2} . dP_S \right) dA - (P_S + dP_S) . (A + dA) - dF \tag{3}$$

where ρ is the density, A the local area, V the volume and P_S the static pressure.

$$\Delta P = \int_c^f \frac{dF}{A} = \int_c^f q . C_F . \frac{g}{A} . dl \tag{4}$$

where dF is the friction force on an element of the boundary, g.dl is an element of the boundary area, q is the dynamic pressure, g the local perimeter along which the friction force is applied and C_f the friction coefficient.

Dividing Eq. (4) by the entry dynamic pressure q_c, using continuity and referring the loss in total pressure to a function of both the approach loss ΔP_a and the duct loss ΔP_d Eq. (5a) is obtained. A comparison of the measured loss coefficients with those given by Eq. (5) would reveal the extent of any lip separation at low speeds and that of pre-entry separations at high speeds. The pressure recovery $\eta_{\sigma I}$, Eq. (5b), represents the duct efficiency in terms of pressure loss.

$$\frac{\Delta P}{q_c} = \int_0^{l_c} \left[\left(\frac{A_c}{A} \right)^2 . C_{Fa} . \frac{g}{A} \right] . dl + \int_{l_c}^{l_f} \left[\left(\frac{A_c}{A} \right)^2 . C_{Fd} . \frac{g}{A} \right] . dl = \frac{\Delta P_a}{q_c} + \frac{\Delta P_d}{q_c} \text{ and } \eta_{\sigma i} = 1 - \frac{\Delta P}{q_\infty} \tag{5a, b}$$

where C_{Fa} is the approach effective friction coefficient and C_{Fd} is the duct effective friction coefficient

EMBRAER ERJ-170 engine installations are podded, so it will be assumed that there is negligible approach loss in cruise, implying that the throat area in Eq. (1) is equivalent to the entry area A_c. The wetted area, or the approach surface, is zero. Figure (3) (Squire, 1947), based on inlet duct conical experiments considering arbitrary section shape diffusers and area variation, gives C_{Fd}. The equivalent cone angle duct is given by Eq. (6a). The drag coefficient C_F depends on the flow characteristics and. is calculated from Eq. (6b, c) for compressible turbulent flows with Reynolds number not greater than 10^9, known as the Schlichting empirical equation with the Prandt-Glauert correction for compressibility effects (Fox, 1995).

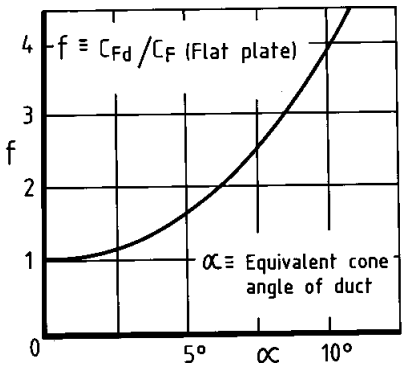

Figure 3 Effective friction in duct

$$\alpha = 2.\tan^{-1}\left[\frac{2.(g_c.A_f - g_f.A_c)}{g_c.g_f.(l_f - l_c)}\right],\ C_F = \frac{0.455.[\log(R_{eff})]^{-2,58}}{(1+0.144.M)^{0,65}} \text{ and } R_{eff} = \frac{4.A_c.V_c}{g_c.\upsilon} \qquad \text{(6a, b, c)}$$

where R_{eff} is the Reynolds effective number for the equivalent flat plate and υ is the fluid viscosity.

The diffuser length, (f-c) in Fig. (2), is estimated iteratively from Eq. (5) and (6) to obtain the best performance relation comprising minimum total length and high pressure recovery.

2.3 Exhaust System

The most important problem concerning the exhaust system design is to match the nozzles exit areas at different altitudes to the necessary thrust. In some cases, it may be required to use nozzle variable geometry. However, for most subsonic civil applications, a simple convergent nozzle can accelerate the exhaust gases efficiently.

An initial nacelle layout is drawn based on the assumption that the exit area is approximately 0.5 to 0.7 times the captured area for a subsonic convergent nozzle. The nozzle arrangement may have a substantial effect on the nacelle external drag, so it is desirable to have an exit cone angle less than 15° and the outside angles of the nozzle be less than 20° in the nozzle-closed position.

Nozzle areas are estimated from engine data performance requirements and its deck. Mass flow was calculated assuming ideal isentropic 1-D flow gas. The nozzle ideal mass flow is given by Eq. (7) as function of the flow properties. However, the actual mass flow is not usually equal to the ideal one, as shown in Eq. (8).

$$\dot{m}_{ideal} = A.\frac{P_T}{\sqrt{T_T}}..\sqrt{\frac{\gamma}{R}}.M.\left[1+\left(\frac{\gamma-1}{2}\right).M^2\right]^{\left[\frac{1+\gamma}{2.(1-\gamma)}\right]} \qquad (7)$$

$$\dot{m}_{real} = C_d.\dot{m}_{ideal} = C_d.(\rho.V.A) \qquad (8)$$

where C_d is the nozzle discharge coefficient

$$M = \sqrt{\frac{2}{\gamma-1}.\left[\left(\frac{P_T}{P_S}\right)^{\left(\frac{\gamma-1}{\gamma}\right)} - 1\right]} \qquad (9)$$

The uninstalled net thrust is the exit gross thrust minus the inlet ram drag, as shown in Eq. (12). The effective velocity, or the fully expanded isentropic velocity, takes into account local compressibility effects, as shown in Eq. (13). The coefficient C_{fg} is the nozzle gross thrust coefficient, which relates the ideal to the actual thrust. C_d and C_{fg} coefficients curves as function of nozzle pressure ratio (NPR) are intrinsically related to the nozzle aerodynamic quality. Further details concerning nozzle coefficients are found in Oates, 1989 and GEAE, 1999a.

$$FN_{total} = FG_{total} - F_{ram} = \left(C_{fg}.\dot{m}_{nozzle}.V_{eff,nozzle}\right) - \left(\dot{m}_{total}.v_{\infty}\right) \tag{10}$$

$$V_{eff} = V + \frac{A}{\dot{m}}.\left(P_{S,nozzle} - P_{S,amb}\right) \tag{11}$$

The nozzle exit areas are calculated iteratively from the nozzle bypass exit area and the resulting gross thrust compared to the required thrust taken from the engine deck to the specific flight conditions. Detailed considerations on engine cycles and aerothermodynamics are found in Oates, 1984.

2.4 Nacelle hardpoints

To start a subsonic nacelle design, it is suggested to set the lip radius in the range of 6 to 10% of the inlet front face radius. To minimize distortion, two different radii are used: 8% for the inner part of the lip and 4% for the outer. Inner lip radius up to 50% greater than the outer radius would reduce the effect of the angle of attack during take-off and landing. In this study, 20 hardpoints were calculated as indicated in Fig. (4) and described below.

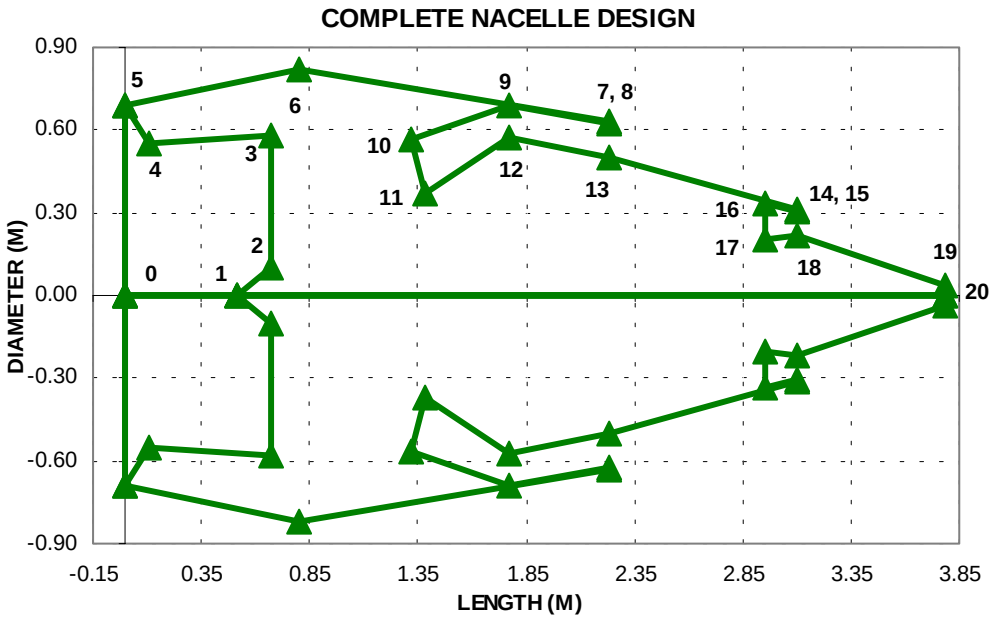

Figure 4. Hardpoints numbering convention

The spinner coordinates, points 1 and 2, are both known from engine dimensions. Point 3 y coordinate is known from the fan radius; its x coordinate is estimated by Eq. (5). Point 4 y coordinate is estimated by Eq. (1). The maximum radius coordinates, point 6, depends on the accessories package maximum radius and was set to 10% greater than this value.

Equations (9) to (13) give the y coordinates difference between points 8-13 and 15-18 (nozzle areas). The outlet guide vanes (OGV) at the bypass entry (points 10 and 11) and the low-pressure turbine (LPT) exit coordinates (points 16 and 17) are engine dimensions. Thrust reverser cowl trailing edge thickness and after core cowl trailing edge are both set to 0,005m. Flow was considered as axial at the high-pressure compressor (HPC) and the LPT. The bypass duct was considered convergent.

Points 18, 19 and 20 are determined having in mind that the after plug angle must be between 10^o and 15^o (the maximum is desirable to minimize the total nacelle length and the minimum to provide minimum loss). The cone angle from the LPT to the plug is usually in the range of 0^o to 7^o. The end plug diameter, a manufacturing requirement, was set to 0.076m.

To calculate points 7, 8, 13, 14, 15 and 18, it was considered that the thrust reverser cowl angle from point 6 (the maximum diameter position), is not greater than 10^o (greater values applied to low subsonic flows), the aft cowl angle is

between 10° and 15° and the nozzle areas and trailing edges thickness are already calculated. The EBU maximum volume criteria design determines, together with the nozzle area restrictions, points 9 and 12 coordinates.

The minimum diameter position was set as 15% of the nacelle chord (from point 5 to points 7, 8) and the leading edge radius as an arithmetic average of the min and max radius to determine point 5.

Nacelle optimization requires the performance analysis at several flight operating conditions. In this work, only a few extreme conditions, like takeoff/top climbing (high thrust, high engine mass flow, very high angle of attack (AOA), low aircraft speed) and maximum cruise (low thrust, low engine mass flow, low angle of attack, high aircraft speed), were chosen to calculate the hardpoints.

2.5 Nacelle aerodynamic design

The nacelle surfaces were drawn smoothly from the calculated hardpoints. Aerodynamic fitting curves were used to reduce drag. The nacelle was divided into two parts: the front cowl, which comprises the inlet, the fan and the thrust reverser cowls and the aft core cowl. For both parts, a maximum radius of curvature was set to prevent large adverse gradient pressures and smooth transitions were applied.

The inlet front cowl has an airfoil profile. The XFOIL software (see Drela, 2001) is an iterative design and analysis tool for subsonic isolated airfoils based on the panel method applied for integral 2-D boundary layers. Although not applied for axis-symmetric problems and compressible flows, it was useful to define the initial profile through points 3, 4, 5, 6, 7 and 8 to be iteratively tested. The chosen profile was the one that supported the highest free flow Mach number before boundary layer separation, attempting to minimize drag.

The aft geometry profile was obtained with CAD tools considering smooth polynomial fitting curves through the hardpoints. Nacelle performance was analyzed using Fluent CFD commercial code (Fluent, 1998), which uses finite volume formulation, cell-centered, to solve the Navier-Stokes equations for unstructured meshes. Second order upwind and explicit time integration were set. Fluent validation and application for aeronautical problems can be found in Fluent, 1998, Mattos, 1999 and Damian, 2002.

3. Results

3.1 Inlet capture radius

The EMBRAER ERJ-170 maximum cruise speed is Mach 0.82. The maximum Mach number at the fan stage was chosen to be 0.65. The engine fan diameter is 1.160m. The inlet capture diameter, calculated from Eq. (1), was D_{throat}=1.105 (A_{throat}=0.9074m^2). Compared to the data shown in Fig. (1), the results are up to 17% higher.

It was also necessary to estimate the diffuser length. Figure (5) shows the fan Mach number influence on the inlet pressure recovery, $\eta_{\sigma i}$. The inlet pressure loss, which directly influences the pressure recovery, has two different sources: the first one is due to the wetted area and its viscous effect on surface; the second is due to the diffuser angle effect (Squire, 1947). So, the pressure loss is directly proportional to both the wetted area and the diffuser angle. However, while the wetted area is directly proportional to the duct length, the diffuser angle is inversely proportional to it and a compromise solution must be found. Hence, for a fan Mach number of 0.65 the diffuser length would be about 0.56m. It is also important to notice the strong influence of the fan maximum Mach number on the pressure recovery. It is clear that any turbomachine improvement in the fan allowing to get higher inlet Mach numbers will provide benefits in terms of $\eta_{\sigma I}$, thrust and fuel consumption. The high-pressure recovery coefficient obtained for the designed inlet ($\eta_{\sigma i}$=99,35%) confirms its good performance. Table (1) resumes the main inlet diffuser results.

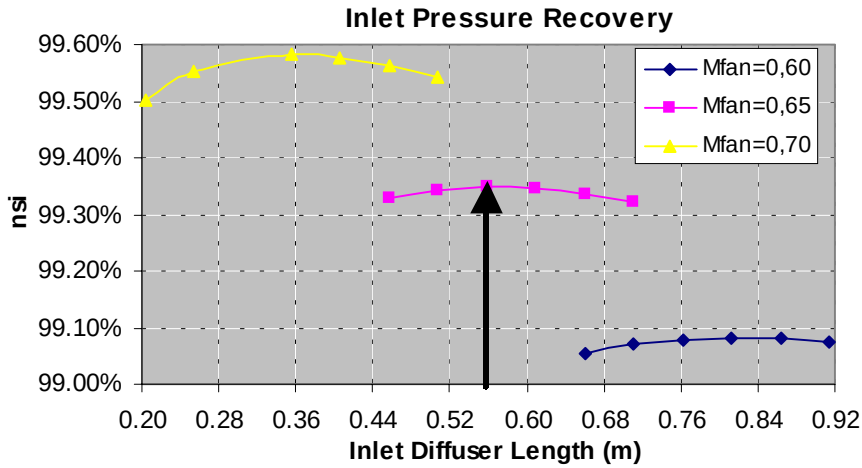

Figure 5. Fan Mach number influence in the inlet diffuser length

Table 1. Results obtained for the inlet radius sizing

Parameter	English Units	SI Units
Inlet Radius	21.75in.	0.5524m
Pressure Loss	0.0096psig	66.49Pa
$\eta_{\sigma I}$ (%)	99.35	99.35
η_{kd} (%)	99.52	99.52
η_{d} (%)	99.80	99.80

3.2. Nozzle areas

There are two exit areas in the ERJ-170 engine: the bypass and the core. This work will focus on two critical conditions, one at take-off, and another at cruise, based on GEAE, 1999b, although it is recommended to test for several other flight conditions. Both of them are referred to the ISA (Ideal Standard Atmosphere) condition (15°C and 101,325Pa at sea level) and detailed in Table (2).

Table 2. Critical conditions to calculate the nozzle exit areas (ISA conditions)

Condition	Mach	Alt. (m)	Alfa (°)	Beta (°)	Description
1	0.82	11,300	4.8	0	Long range cruise, max continuous
2	0.20	400	24	0	Climb one engine inoperative

Bypass and core exit areas were calculated from the two conditions above using the engine deck information. The results are shown in Table (3) and are in agreement with experimental data taken from Raymer, 1999 (0.48 to 0.67m^2).

Table 3. Results obtained for nozzle exit areas (ISA conditions)

Position	Area (m^2)	Thrust Margin (%)	BPR
Bypass	0.4413	0.00	5.71
Core	0.1397	6.08	5.83
Total	0.5810	-	-

3.3. Nacelle Design

The 20 nacelle points could be fixed after calculating the inlet radius, the outlet areas and the engine dimensions and compared with existing data (Fig. (6)).

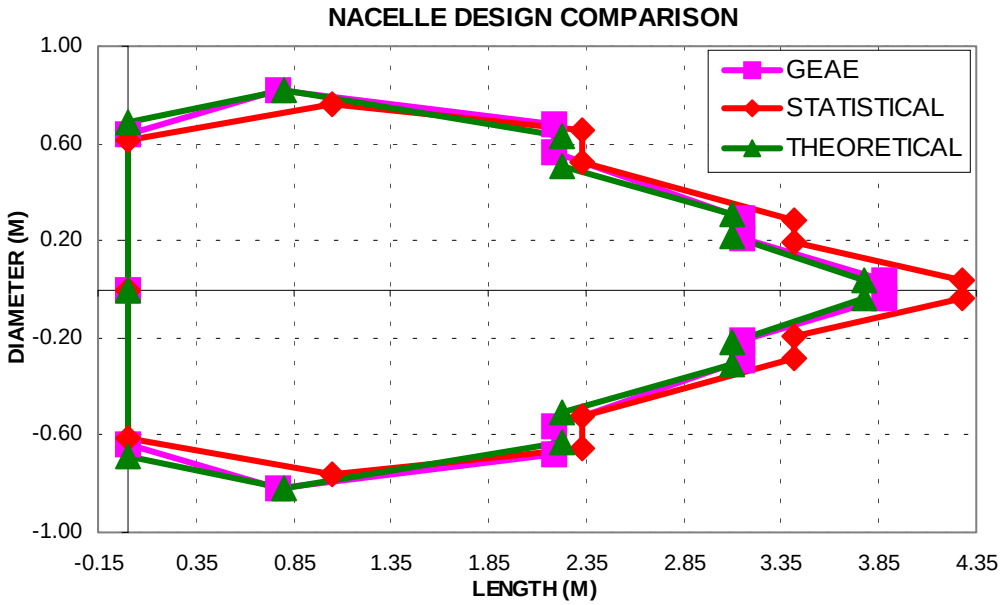

Figure 6. Results comparison

The inlet profile, comprising points 3 to 8, was drawn using beta-spline fitting curves with maximum curvature radius, similar to an airfoil. The curves were then aerodynamically analyzed and optimized in the XFOIL software for

Mach number 0.42 and angle of attack 4.8° conditions. The results show that the pressure distribution was reasonable and did not overpass $C_{P,\,limit} = -3.30$. The pressure peaks noticed in the region from 0.3 to 0.5% of the mean chord, as shown in Fig. (7), were removed with a slightly and non-perceptive change in the initial profile, to avoid very high pressure gradients or shock waves, to maintain the external flow around the nacelle and to keep the calculated hardpoints positioning to assure the correct engine properties. The resulting profile is shown in Fig. (8).

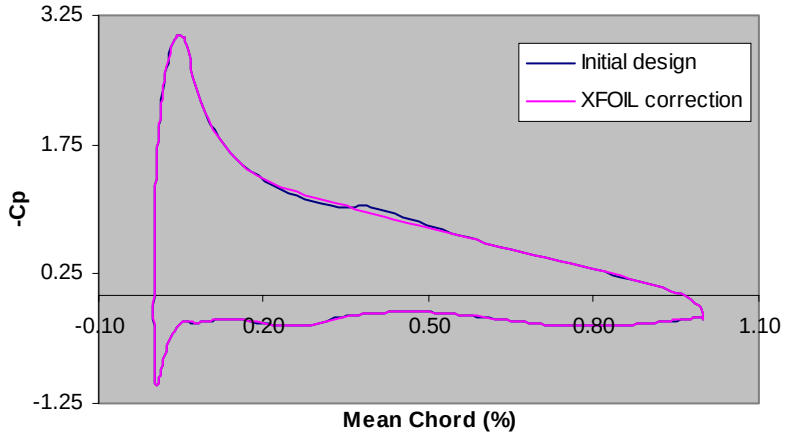

Figure 7. Characteristic of the inlet profile

Figure 8. Initial inlet profile

Beta-spline fitting curves with maximum curvature radius were also used to draw the exhaust profile. The lofting curve was assumed to be orthogonal to the bypass and to the core exit ducts (points 10-11 and 16-17, respectively) to obtain smooth surfaces for the exhaust ducts (the bypass and the core ducts).

Finally, the full nacelle profile, comprising the inlet and the exhaust systems, is generated. Some hardpoints coordinates previously calculated had to be slightly changed for the sake of convergence the aerodynamic design. However, these changes were marginal, as shown in Table 4, and did not affect the main characteristics of the nacelle. The final nacelle configuration is shown in Figure 9. Points 5, 6 and 9 had larger changes.

Table 4. Nacelle adjusted hardpoints

Point	L_{adj} (mm)	Delta L (mm)	R_{adj} (mm)	Delta R (mm)
0	0	0	0	0
1	511	0	0	0
2	670	0	101	0
3	670	0	579	-1
4	114	3	552	-1
5	-40	-40	631	-56
6	692	-110	819	-1
7	2231	0	632	-1
8	2231	0	627	-1
9	1770	0	698	10
10	1315	-6	567	0
11	1377	-3	368	0
12	1770	0	577	0
13	2231	0	503	0
14	3101	0	310	0
15	3101	0	305	0
16	2956	0	333	0
17	2956	0	202	0
18	3101	0	220	0
19	3781	0	38	0
20	3781	0	0	0

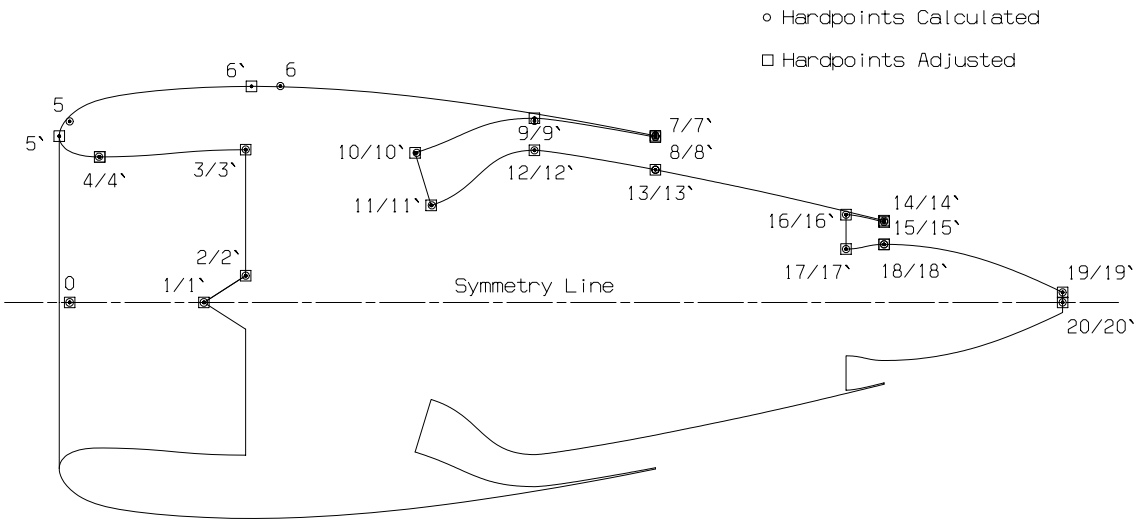

Figure 9. Complete Nacelle Designed

3.5 CFD Analysis

Two ERJ-170 nacelle models were analyzed: an axis-symmetric one for condition 1 (high speed) and a bi-dimensional one for condition 2 (high AOA). A 200,000 quadrilateral elements axis-symmetric mesh was built. The realizable k-ε turbulence model (Fluent, 1998) with wall function treatment was used. Boundary layer refinement was obtained with about 20 nodes, the first one being at Y^+~62 (low-Reynolds number is not suitable to this problem). The results in Fig. (10) to (13) show that condition 1 is more critical than condition 2. The nacelle simulated is a little different from Fig. (9), because at the time the simulation was done, points 9 and 12 in the bypass duct were not set.

Problems were detected like strong shock waves in the outer inlet cowl, with a diamond configuration (compression and expansion) formed in the core cowl. Therefore, external drag increase and boundary layer thickness raise, which may cause separation flow, already detected in the thrust reverser cowl trailing edge, were expected. Inlet distortion in the internal engine flow is also a problem to pay attention. Bypass duct exit nozzle is choked and thick mixing layers in both trailing edges (thrust reverser and aft core cowls) may cause heat losses and noise.

Some changes are proposed for future iterations: to decrease the relative inlet profile thickness, keeping the main hardpoints at the same position, and to reduce the thrust reverser cowl, the aft core cowl and the plug angles.

It is expected that the improvement of the designed nacelle in Fig. (9) would reach the actual results for the Mach number distribution, shown in Fig. (14).

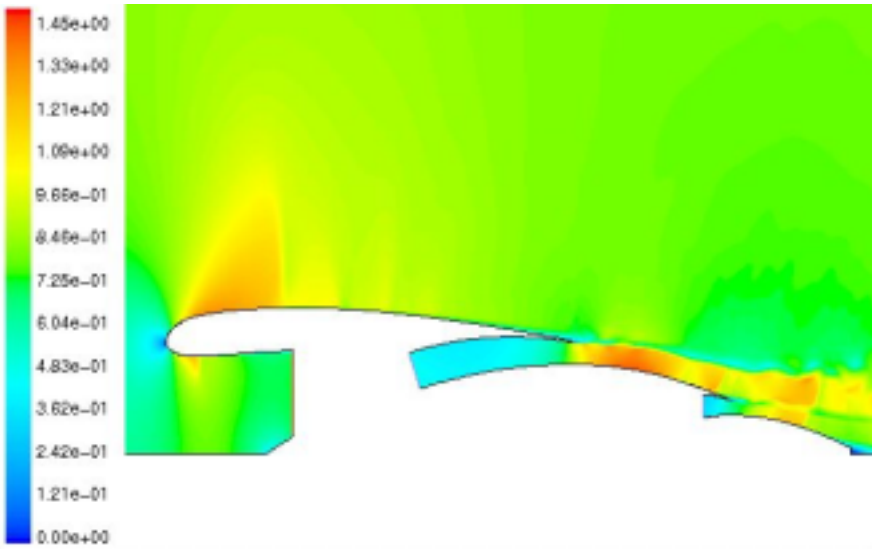

Figure 10. Nacelle Mach number distribution for cruise

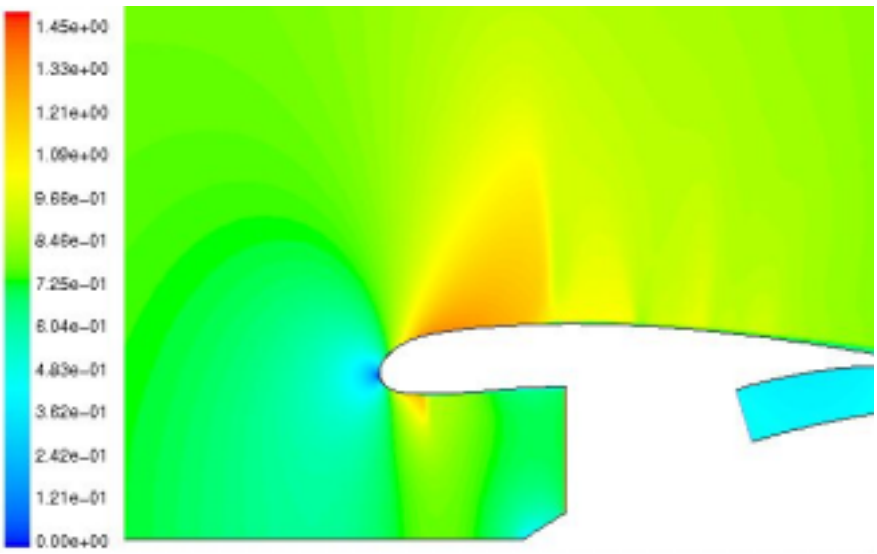

Figure 11. Nacelle Mach number distribution for cruise

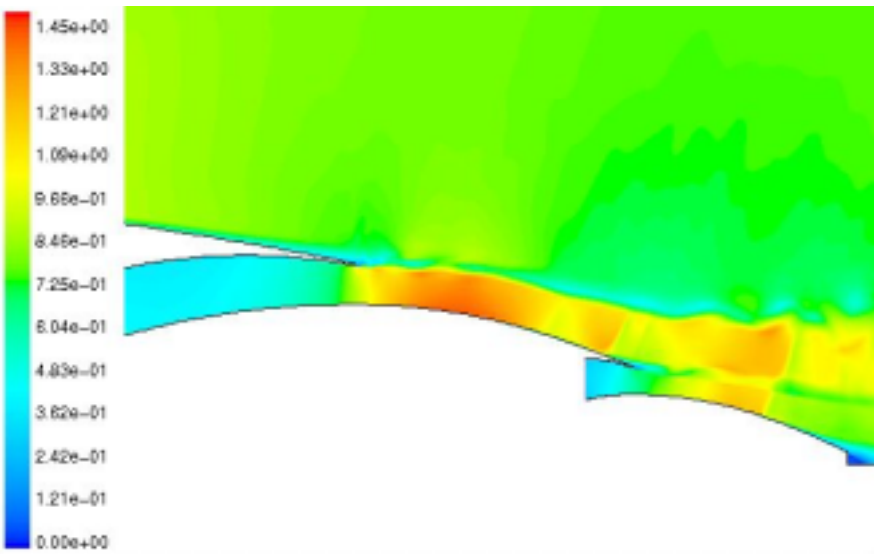

Figure 12. Nacelle exhaust system Mach number distribution for cruise

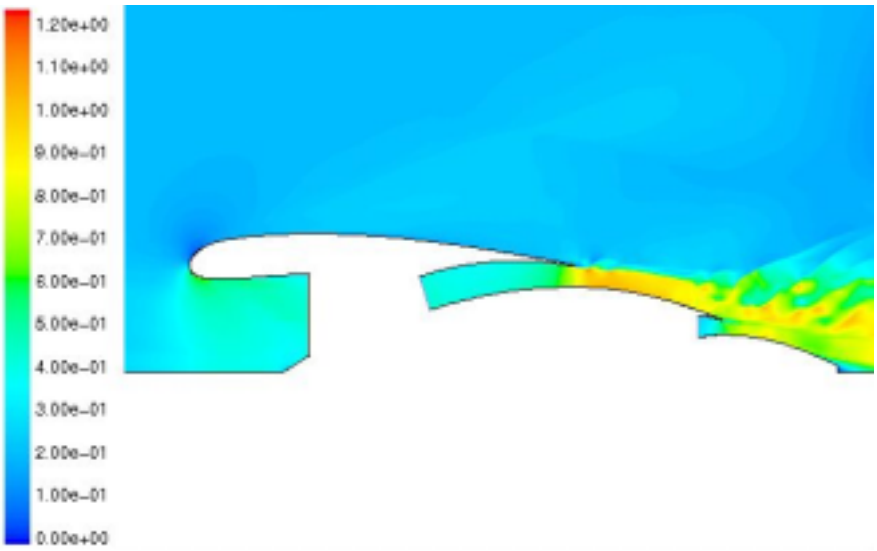

Figure 13. Nacelle Mach number distribution for take off

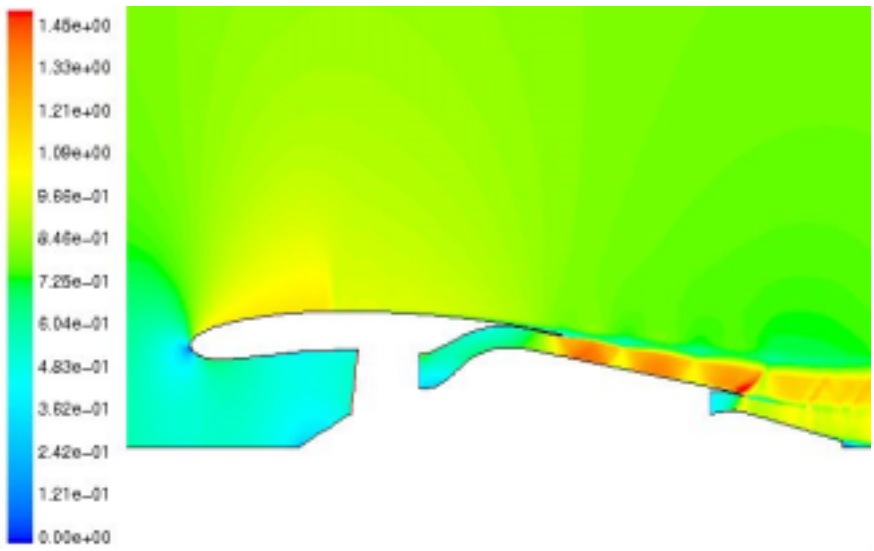

Figure 14. EMBRAER ERJ-170 nacelle Mach number distribution

4. Conclusion

The new methodology to design subsonic nacelles proposed in this paper was applied to the EMBRAER ERJ-170 aircraft. The results, when compared to the existing nacelle, indicate that the methodology is acceptable and may lead to a shorter nacelle. The inlet and the outlet areas hardpoints were determined from the momentum and mass conservation equations. Further assumptions concerning engine characteristics determined the remaining hardpoints. The nacelle profile was drawn in CAD using smooth profiles fitted to the calculated hardpoints. A suitable aerodynamic analysis was done in the XFOIL for the initial inlet profile to prevent pressure peaks. A CFD analysis completes the work, checking the methodology and improving the nacelle performance.

The methodology is more accurate than the statistical ones because it uses more realistic data. It may be applied to draw more suitable nacelle profiles and to maintain expected performance, without undesired characteristics that would disturb the flow delivered to the engine and the external flow around the supporting structure. Pressure distribution has been calculated and used to optimize nacelle performance through inlet profile redrawing, which means to avoid separation and to decrease the drag.

From the CFD analysis, it is possible to foresee problems and to correct them. The nacelle profile design is an iterative and time-consuming process. As a continuation of this work, additional flight conditions may be tested. Next iterations should focus on trying to redraw thinner leading edges and smaller thrust reverser, aft core and plug cowl angles to minimize loss of performance at climb angles of attack.

5. References

Brodt, C.S., 2001, “Design and Integration of Nacelles for Aeronautical Engines”, ITA Under-Graduation Project, São José dos Campos, SP, Brazil, 118p

Damian, R.B., 2002, “Estudo Comparativo de Códigos Comerciais de CFD na Solução de Problemas Simples de Escoamentos Compressíveis e Incompressíveis”, ENCIT Paper number 02-0675, Brazil, 12p

Drela, M., Youngren, H., 2001, “XFOIL 6.9 User Guide”, 33p

Fluent Inc., 1998, “Fluent 5 User´s Guide”, 4 Volumes

Fox, R.W., McDonald, A.T., 1995, “Introdução à Mecânica dos Fluidos”, 4ª Edição, Ed. Guanabara Koogan S.A., 662p

GEAE, 1999a, “ERJ-170/CF34-8E Core Nozzle Thrust Coefficient”, EMBRAER

GEAE, 1999b, “ERJ-170/CF34-8E Isolated Nacelle Performance”, EMBRAER

GEAE, 2001, “ERJ-170/CF34-8E Propulsion System Familiarization Training”, EMBRAER

Hill, P.G., Peterson, C.R., 1970, “Mechanics and Thermodynamics of Propulsion”, 3rd print, Addison-Wesley

Mattingly, J.D., Heiser, W.H., Daley, D.H., 1987, “Aircraft Engine Design”, AIAA Education Series

Mattos, B. S. de, et all: “Transonic Euler Flow Calculation Around a Transport Configuration with Powered Engine Effects”, AIAA Paper number 99-0529, USA

Oates, G.C., 1984a, “Aerothermodynamics of Aircraft Engine Components”, USA

Oates, G.C., 1984b, “Aerothermodynamics of Gas Turbine and Rocket Propulsion”, USA

Oates, G.C., 1989, “Aircraft Propulsion Systems Technology and Design”, AIAA, Washington DC, USA, 528p

Raymer, D.P., 1999, “A conceptual approach”, 3rd Ed., Washington D.C., USA

Roskam, J., 1997, “Airplane Design Vol. II: Preliminary configuration and integration of the propulsion system”, USA.

Seddon, J., Goldsmith, E.L., 1985, “Intake Aerodynamics”, AIAA, Washington, D.C., 442p

Squire, H.B., 1947, “Experiments on Conical Diffusers”, RAE Aero 2216